Int. J. Heat Mass Transfer. Vol. 22, pp. 1525–1532.

0017–9310/79/1101–1525 $02.00/0

A THEORETICAL INVESTIGATION OF HEAT TRANSFER IN A LADLE OF MOLTEN STEEL DURING POURING

P. EGERTON, J. A. HOWARTH and G. POOTS
Department of Applied Mathematics, University of Hull, HU6 7RX, England

and

S. TAYLOR-REED
British Steel Corporation, Scunthorpe, England

(*Received* 15 *June* 1978 *and in revised form* 23 *January* 1979)

Abstract—A theoretical model is proposed for the flow and heat transfer of molten steel in a ladle during pouring. Analytical and numerical solutions are obtained. Within the limitations of the model, agreement with plant observations is satisfactory.

NOMENCLATURE

a, radius of ladle;
A_L, cross-sectional area of ladle;
A_N, cross-sectional area of nozzle;
Bi, Biot number;
C_N, nozzle contraction factor;
g, gravitational acceleration;
$h(t)$, head of steel at time t;
H, initial head of steel;
$\bar{h}$, heat transfer coefficient;
K, thermal conductivity;
k, thermal diffusivity;
P, Prandtl number;
(r,z), cylindrical polar coordinates;
R,y,Z, dimensionless coordinates;
t, time;
$t_f = \dfrac{A_L}{A_N C_N}\sqrt{2H/g}$, emptying time;
T, temperature;
T_1, initial temperature.

Greek symbols

α, $= H/a$, aspect ratio of ladle;
δ, thermal boundary layer thickness;
ε, $= kt_f/H^2$, dimensionless emptying time;
θ, $= (T-T_0)/(T_1-T_0)$, normalized dimensionless temperature;
ν, kinematic viscosity;
ρ, density;
$\hat{\tau} = kt/H^2$, $\tau = t/t_f$, dimensionless times.

Subscripts

0, ambient condition;
1, wall condition;
2, slag condition;
F, fusion;
f, final emptying condition;
N, nozzle condition;
s, standing condition.

1. INTRODUCTION

THE LADLE (see Fig. 1) is essential to the operation of a modern integrated iron and steel plant. It is a refractory-lined steel vessel, typically holding 300 tonnes of liquid metal. It is used to transport iron or steel in molten form with a minimum of heat loss and also to pour steel into moulds prior to solidification and further processing.

This paper is concerned only with the most common method of pouring, through an off-centre nozzle built into the ladle base. The pouring process for a single ladle (termed a *cast* of steel) can take up to 60 min. This is preceded by the transfer of the steel in the ladle from the steelmaking plant to the pouring station, which can also take up to 60 min. The initial temperature of the steel before these stages is of the order of 1600°C; thus there will be considerable heat transfer from the steel, and temperature stratification may occur. For reasons of product quality, the steel temperature during the pouring sequence (termed the *teem*) must fall within a closely specified temperature range (as little as ± 5°C for certain steels). Thus it is important to have a method for predicting the temperature variation throughout the cast. Quantitative information on the average pouring temperature and its variation can have significant benefits for the steel plant. The effects of variations in process routes, such as times, filling temperatures, slag cover, insulating materials, initial thermal state of the ladle etc. can be studied, and the cost-benefits of amended conditions or improved materials can be evaluated.

This paper examines theoretically the temperature distribution and flow of steel within a ladle during transfer and pouring. Previous work on this problem includes experimental simulations by Hlinka [1] using water in an acrylic cylinder, with a top layer of oil to represent slag insulation cover. The effect of molten slag thickness on the heat loss from the top surface of molten steel in a ladle has been in-

vestigated theoretically by Szekely and Lee [2], but this work is not concerned with the flow and heat transfer during the actual pouring sequence.

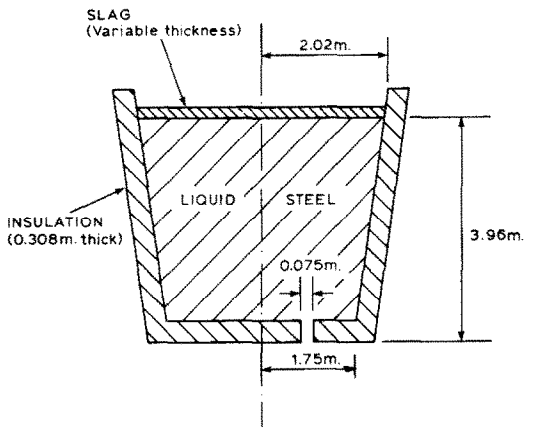

FIG. 1. Teeming ladle.

It is the purpose of this preliminary investigation to construct a simple mathematical model of ladle pouring and heat transfer which gives insight into the physical processes which occur, and which indicates any further modifications to be made to the model so as to simulate more exactly the real situation. The prime objective in constructing such a model is the prediction of the nozzle streaming temperature.

The basic assumptions made are as follows:

(i) In order to predict the heat transfer within the ladle during pouring, it suffices to assume that the flow of the molten steel is inviscid and irrotational.

As the ladle empties, transient viscous and thermal boundary layers are attached to the inner walls of the ladle. Now since the Prandtl number $P = \nu/k = 0.08$ for molten steel, it follows that the thickness δ_T of the thermal boundary layer at any location will be greater than the thickness δ_H of the corresponding hydrodynamic boundary layer; this follows from the observation that in any such high Reynolds number forced convection flow, for small Prandtl number, the ratio $\delta_T/\delta_H = O(P^{-1/2})$. Hence an inviscid flow approximation is made in the calculation of the ladle temperature. The error involved can be estimated. It will be shown that the fall in nozzle temperature is small and of $O(kt_f/H^2)$, where t_f is the pouring time of the ladle. For a typical value of t_f of 1 hr, $kt_f/H^2 = 1.6 \times 10^{-3}$. Consequently the effect of viscosity, for high Reynolds number flow, will be of second order, namely $O(P^{-1/2}kt_f/H^2)$. It can also be argued that, bearing in mind the large scale dimensions of the ladle, the effects of viscosity are negligible in the emptying process, except when the ladle is almost empty.

(ii) The thermal capacity and thickness of the refractory walls are ignored and it is assumed that the thermal condition at the inner ladle/slag surface can be represented by

$$K \left.\frac{\partial T}{\partial n}\right|_B = -\bar{h}_B(T - T_0). \tag{1.1}$$

Here T_0 is the ambient air temperature, $\bar{h}_B$ the heat transfer coefficient at the molten steel boundary and n is measured outwards along the normal from the steel volume. An overall averaged value of $\bar{h}_B$ relevant to the inner ladle surface (and also one for the slag/steel interface) is available from an analysis of plant data obtained from a variety of operating conditions.

It should be emphasised that it is possible to include the transient heat transfer at the ladle wall in the model. However, this idealization is made in order to simulate, in an overall sense, a wide variety of conditions that may exist in a typical working day of a steel plant. For example, prior to filling the ladle it may be cold, preheated, or warm from a previous teem. (However it is always desirable to ensure that the ladle wall is sufficiently hot to prevent solidification of the steel during the pouring process.)

(iii) It is assumed that the effect of ladle taper on heat transfer is small. Thus the ladle is represented by a circular cylinder having a (mean) radius $(a_T + a_B)/2$, where a_T and a_B are respectively the top and bottom inner ladle radii.

The relevant measure of the taper is in fact small, this being the dimensionless group $(a_B/H)s$, where $s = (a_T/a_B) - 1$ and its value is $s = 0.15$.

It will be seen later that the reasons for neglecting ladle taper, in relation to the *mathematical* formulation, are two fold. First the fluid velocity of the molten steel, on the basis of an inviscid approximation, will be vertically downwards and equal in magnitude to the rate at which the top (slag covered) surface falls. Thus it will be a function of time only, and independent of the height z measured upwards from the ladle base. Secondly, because of this idealization and assumption (1.1), the thermal field can be separated into radial and axial variations, and this enables analytical and numerical solutions readily to be obtained.

The error in the heat transfer due to the neglect of ladle taper can be shown to be $O(skt_f/H^2)$, i.e. of second order, as is the neglect of viscosity.*

(iv) Finally it is assumed that the physical properties of the molten steel are independent of the temperature (see Table 1).

The actual variation in these quantities is small over the relevant range of temperature, say between 1550 and 1600°C. Once again the assumption makes the problem more tractable in the mathematical sense. It does imply, however, that motion induced by the gravitational body force is neglected. In this connection it may be noted that at the base of the ladle, there is a state of stable thermal stratification.

* The relevant analysis required to derive this result is not presented here; in fact it follows closely that given in Section 3.

Table 1. Thermal properties of liquid steel

Density	$7510\,\mathrm{kg\,m^{-3}}$
Specific heat	$700\,\mathrm{J\,kg^{-1}K^{-1}}$
Viscosity	$48\times10^{-4}\,\mathrm{Ns\,m^{-2}}$
Conductivity	$29\,\mathrm{W\,m^{-1}\,K^{-1}}$
Heat transfer coefficient (Ladle walls, bottom)	10–$30\,\mathrm{W\,m^{-2}\,K^{-1}}$
Heat transfer coefficient (Slag cover)	1–$15\,\mathrm{W\,m^{-2}\,K^{-1}}$
Diffusivity ($K/\rho c$)	$5.71\times10^{-6}\,\mathrm{m^2\,s^{-1}}$
Fusion temperature of steel	1470–1530°C

Buoyancy forces may not be negligible in the region adjacent to the (vertical) ladle walls. However this region of thermal stratification is small in comparison with the radius of the ladle, and dimensional arguments show that any buoyancy driven upflow there will have little effect on the overall downflow.

Subject to the above assumptions, the equations governing the flow and heat transfer are formulated in Section 2. In Section 3, a solution of these equations is obtained for the special case of no thermal stratification at the beginning of the pouring sequence (by means of the method of matched asymptotic expansions). When the ladle is nearly empty this solution is invalid. The nature of the mathematical structure near to this final time can be revealed (for example, by employing the approximate heat balance integral method). However, as the fluid model breaks down at this time, these details will be omitted. In Section 4 the general case of thermal stratification existing prior to the pouring sequence is examined by numerical methods. A comparison is then made in Section 5 between analytical and numerical solutions, as is a comparison with available plant observations. Conclusions are given in Section 6.

2. FORMULATION

Consider first the inviscid fluid flow of the molten steel within the ladle during the pouring sequence. Let the cross-sectional area of the cylindrically shaped ladle be denoted by A_L, and that of the nozzle be A_N, where $A_N \ll A_L$. The contraction factor of the nozzle (to account for the inward bending of the streamlines towards the vertical axis) is denoted by C_N. Let the initial head of molten steel be denoted by H and during the pouring sequence let the height of the top surface be located at $z = h(t)$. Using the equation of conservation of mass and Bernouilli's equation it is a straightforward matter to show that:

$$\frac{\mathrm{d}h}{\mathrm{d}t} = \frac{-2H}{t_f}\left(1-\frac{t}{t_f}\right), \quad h(0) = H. \tag{2.1}$$

Here t_f is the final emptying time for the ladle and is given by:

$$t_f = \frac{A_L}{A_N C_N}\sqrt{\frac{2H}{g}}, \tag{2.2}$$

where g is the gravitational acceleration. Integration of equation (2.1) yields the result

$$\frac{h(t)}{H} = \left(1-\frac{t}{t_f}\right)^2. \tag{2.3}$$

To simulate (for the ladle geometry described in Section 1) an observed emptying time of 1 hr, the contraction factor C_N must take the value 0.633.

In terms of cylindrical polar co-ordinates (r, θ, z) the inviscid irrotational flow of the molten steel has velocity components:

$$\mathbf{v} = (v_r, v_\theta, v_z) = \left(0, 0, \frac{\mathrm{d}h}{\mathrm{d}t}\right), \tag{2.4}$$

and during pouring the equation governing heat conduction and convection reduces to:

$$\frac{\partial T}{\partial t} - \frac{2}{t_f}\left(1-\frac{t}{t_f}\right)\frac{\partial T}{\partial z} = k\left(\frac{1}{r}\frac{\partial}{\partial r}\left(r\frac{\partial T}{\partial r}\right)+\frac{\partial^2 T}{\partial z^2}\right). \tag{2.5}$$

Here T is the temperature and k is the thermal diffusivity. For the waiting period prior to pouring the temperature will be governed by the heat conduction equation, i.e. as in equation (2.5) with the convective heat transfer term omitted. It will be seen that, because of the time scales involved, such thermal stratification is more in the nature of transient boundary layers attached to the walls rather than a change in the bulk (or core) of the molten steel from the initial filling temperature T_1.

To understand the mechanisms controlling the heat transfer in the steel only the case of no thermal stratification at the onset of pouring will be considered in this section. The general case of thermal stratification prior to pouring is considered in Section 4.

Here the initial condition will be taken as:

$$T = T_1 \text{ for } 0 \leqslant z \leqslant H,\ 0 \leqslant r \leqslant a, \text{ at } t = 0, \tag{2.6}$$

where a is the radius of the ladle. As previously indicated, in order to model the loss of heat through the walls and slag covered surface, a Newton cooling law is assumed. Thus for $t > 0$:

$$K\frac{\partial T}{\partial z} = -\bar{h}_2(T-T_0) \quad \text{at } z = h(t),\ 0 \leqslant r \leqslant a. \tag{2.7}$$

$$K\frac{\partial T}{\partial z} = \bar{h}_1(T-T_0) \quad \text{at } z = 0,\ 0 \leqslant r \leqslant a, \tag{2.8}$$

and on the cylindrical surface

$$K\frac{\partial T}{\partial r} = -\bar{h}_1(T-T_0) \quad \text{at } r = a,\ 0 \leqslant z \leqslant h(t). \tag{2.9}$$

In the above, K denotes the thermal conductivity and $\bar{h}_1$ and $\bar{h}_2$ ($\bar{h}_1 \gg \bar{h}_2$) denote the heat transfer coefficients, at the ladle wall and slag surface respectively, and are available from plant data.

It is convenient to introduce the non-dimensional variables:

$$Z = z/H,\ R = r/a,\ \tau = t/t_f,\ \varepsilon = kt_f/H^2 \quad \text{and } \theta = (T-T_0)/(T_1-T_0). \tag{2.10}$$

The governing equations (2.5)–(2.9) become:

$$\frac{\partial\theta}{\partial\tau}-2(1-\tau)\frac{\partial\theta}{\partial Z}=\varepsilon\left[\frac{\partial^2\theta}{\partial Z^2}+\frac{\alpha^2}{R}\frac{\partial}{\partial R}\left(R\frac{\partial\theta}{\partial R}\right)\right], \quad (2.11)$$

$$\theta=1, \tau=0, 0\leqslant Z\leqslant 1, 0\leqslant R\leqslant 1, \quad (2.12)$$

$$\frac{\partial\theta}{\partial Z}=-Bi_2\theta \text{ at } Z=(1-\tau)^2, 0\leqslant R\leqslant 1, \quad (2.13)$$

$$\frac{\partial\theta}{\partial Z}=Bi_1\theta \quad \text{at } Z=0, 0\leqslant R\leqslant 1, \quad (2.14)$$

$$\frac{\partial\theta}{\partial R}=-\frac{Bi_1}{\alpha}\theta \text{ at } R=1, 0\leqslant Z\leqslant(1-\tau)^2. \quad (2.15)$$

In terms of the representative length scale H the surface Biot numbers are

$$Bi_1=\frac{H\bar{h}_1}{K} \quad \text{and} \quad Bi_2=\frac{H\bar{h}_2}{K};$$

α is the height to radius aspect ratio H/a.

For the ladle dimensions given in Section 1 the aspect ratio $\alpha=2$; the ladle surface Biot number lies in the range $1\leqslant Bi_1\leqslant 5$, whilst that for the slag surface is in the range $0.1\leqslant Bi_2\leqslant 1$. The non-dimensional time ε, corresponding to an actual pouring time of 1 hr, is small and is of order 1.6×10^{-3}. Moreover it is essential to note that it is small compared with the non-dimensional time taken for the molten steel to cool down to its fusion temperature, which is, of course, the minimum temperature possible in any pouring sequence. Consequently in the delay period prior to pouring, which is of the same order as the pouring time, the degree of thermal stratification must be small. Clearly the observed decrease in nozzle streaming temperature must be primarily controlled by the convective heat transfer term of equation (2.11). For example near the base the thermal gradient will be positive and so the convective term retards the rate of cooling compared with that due to thermal diffusion alone. On the other hand in the neighbourhood of the moving slag surface the thermal gradient is negative and so the rate of cooling will be comparatively enhanced.

Since the above boundary conditions (2.13)–(2.15) are homogeneous in θ, the thermal field is separable in the form:

$$\theta(R, Z, \tau; \varepsilon)=U(R, \tau; \varepsilon)V(Z, \tau; \varepsilon). \quad (2.16)$$

Consider first the R-variation. This satisfies the equation

$$\frac{\varepsilon\alpha^2}{R}\frac{\partial}{\partial R}\left(R\frac{\partial U}{\partial R}\right)=\frac{\partial U}{\partial\tau}, 0\leqslant\tau\leqslant 1, \quad (2.17)$$

subject to the boundary conditions:

$$\frac{\partial U}{\partial R}=\frac{-Bi_1}{\alpha}U, \quad R=1, \quad (2.18)$$

and as $\varepsilon\ll 1$,

$$U\to 1 \quad \text{as} \quad R\to 0, \quad (2.19)$$

and the initial condition

$$U=1 \quad \text{at} \quad \tau=0, \quad 0\leqslant R\leqslant 1. \quad (2.20)$$

Secondly for the Z-variation, there results the equation

$$\frac{\partial V}{\partial\tau}-2(1-\tau)\frac{\partial V}{\partial Z}=\varepsilon\frac{\partial^2 V}{\partial Z^2}, 0\leqslant\tau\leqslant 1, \quad (2.21)$$

subject to the boundary conditions:

$$\frac{\partial V}{\partial Z}=-Bi_2V \quad \text{at} \quad Z=(1-\tau)^2, \quad (2.22)$$

$$\frac{\partial V}{\partial Z}=Bi_1V \quad \text{at} \quad Z=0, \quad (2.23)$$

and the initial condition

$$V=1 \quad \text{at} \quad \tau=0, 0\leqslant Z\leqslant 1. \quad (2.24)$$

The function $U(R, \tau; \varepsilon)$, determined by equations (2.17)–(2.20), correct to order ε, is given by:

$$U(R,\tau;\varepsilon)=1-\frac{2\varepsilon Bi_1}{\alpha}\times\left\{\left(\frac{\alpha\tau}{\pi\varepsilon}\right)^{1/2}\exp[-(1-R)^2/4\alpha^2\varepsilon\tau]-\frac{(1-R)}{2\varepsilon}\operatorname{erfc}[(1-R)/2\alpha\sqrt{\varepsilon\tau}]\right\}, \quad (2.25)$$

see Carslaw and Jaeger [3]. As a consequence the thermal radial boundary layer can penetrate at most a distance $(1-R)=O(\alpha\sqrt{\varepsilon})$. For a typical pouring sequence this is equivalent to a thermal stratification over a region of the order of 8% of the radius of the ladle.

As far as the function $V(Z, \tau; \varepsilon)$ (defined by equations (2.21)–(2.24)) is concerned, the mathematical structure is more complex. This is because of the presence of the convective term and the fact that ε multiplies the highest derivative in equation (2.21). In the next section a solution is obtained for the simplest case of an insulated slag surface, $Bi_2=0$. The method of matched asymptotic expansions is employed yielding a uniformly valid solution for pouring times up to $\tau=1-O(\varepsilon^{1/3})$.

Finally it should be pointed out that on the basis of an inviscid flow model and the other assumptions mentioned, the problem of flow and heat transfer in a ladle has been simplified to the problem of determining V, a function of one space coordinate and time. The same comment applies to the general case of cooling prior to pouring, and this is investigated by standard numerical methods in Section 4.

3. THE SPECIAL CASE OF AN INSULATING SLAG SURFACE, $Bi_2 = 0$

In this special case the equations to be solved are (2.21)–(2.24) but with $Bi_2 = 0$. This is a singular perturbation problem, with a four region structure in the (Z, τ) plane. Firstly there is a boundary layer at $Z = 0$, of thickness $O(\varepsilon)$, but also it is found that the solution at small values of τ, in fact $\tau = O(\varepsilon)$, is different from that at $\tau = O(1)$, and two expansions are required. Thus there are four regions.

Region 1: Here τ is $O(\varepsilon)$ and Z is $O(1)$. Hence the new variables are $Z = Z$, $\tau^* = \tau/\varepsilon$, with $V = V^*(Z, \tau^*)$.

Region 2: This is the inner small time region, so that the appropriate variables are $\bar{Z} = Z/\varepsilon$, $\tau^* = \tau/\varepsilon$, with $V = \bar{V}^*(\bar{Z}, \tau^*)$.

Region 3: In the outer spatial region, when τ is $O(1)$, the variables will be the original Z, τ, V.

Region 4: The inner spatial region, with $\tau = O(1)$, requires the variables $\bar{Z} = Z/\varepsilon$, $\tau = \tau$, with $V = \bar{V}(\bar{Z}, \tau)$.

The method of matched asymptotic expansions can be used to determine two term solutions, valid in each of the four regions. The details are not presented here, but the matching may easily be verified (virtually on inspection), and the solutions may just as easily be verified by substitution into the governing equations (cast, of course, in the appropriate variables). The solutions for the four regions turn out to be

$$V^* = 1 + O(\varepsilon^2), \tag{3.1}$$

$$\bar{V}^* = 1 + \frac{\varepsilon Bi_1}{4}\left\{(1 + 2\bar{Z} + 4\tau^*)\operatorname{erfc}\left[\frac{\bar{Z}}{2\sqrt{\tau^*}} + \sqrt{\tau^*}\right] - \exp(-2\bar{Z})\operatorname{erfc}\left[\frac{\bar{Z}}{2\sqrt{\tau^*}} - \sqrt{\tau^*}\right] - 4\sqrt{\frac{\tau^*}{\pi}}\exp\left(-\left[\frac{\bar{Z}}{2\sqrt{\tau^*}} + \sqrt{\tau^*}\right]^2\right)\right\} + O(\varepsilon^2), \tag{3.2}$$

$$V = 1 + O(\varepsilon^2), \tag{3.3}$$

and

$$\bar{V} = 1 - \frac{\varepsilon Bi_1}{2(1-\tau)}\exp[-2(1-\tau)\bar{Z}]. \tag{3.4}$$

The required results for the nozzle streaming temperature, obtained by evaluating the above at $\bar{Z} = 0$, are:

$$\frac{(T_N - T_0)}{(T_1 - T_0)} = 1 + \tfrac{1}{2}\varepsilon Bi_1\left\{2\tau^* - (1 + 2\tau^*) \times \operatorname{erf}\sqrt{\tau^*} - 2\sqrt{\frac{\tau^*}{\pi}}\exp[-\tau^*]\right\} \tag{3.5}$$

for $\tau = O(\varepsilon)$, and

$$\frac{(T_N - T_0)}{(T_1 - T_0)} = 1 - \varepsilon Bi_1/2(1 - \tau), \tag{3.6}$$

for $\tau = O(1)$.

It might be pointed out at this stage that it is very easy to add a boundary layer at the top, to account for the case $Bi_2 \neq 0$; this does not need the sophistication of two temporal regions. However, this does not affect the nozzle temperature, except when τ is very close to unity, and the top boundary layer "collapses" on to the bottom one. In fact, near $\tau = 1$, the above solution is clearly invalid. (The formal mathematical structure can be elucidated, and it turns out to be in a region when $1 - \tau = O(\varepsilon^{1/3})$. However, since the model is inadequate in this very small temporal region, this formal exercise is not presented.)

In Section 5, the above analytical solutions for an insulating slag surface are shown to be in exact agreement with numerical solutions of the equations. This verification proved invaluable in checking computer algorithms involved in the study of the general case with thermal stratification prior to pouring.

4. NUMERICAL SOLUTIONS

For a typical waiting period of 1 hr, for the ladle geometry described in Section 1, the zone of radial thermal stratification is insufficient to affect the nozzle streaming temperature. However the thermal stratification rising from the base and that attached to the slag interface is important in this connection.

Thermal stratification prior to pouring

Let t_s be the standing time prior to pouring; further let

$$\hat{\tau} = \frac{kt}{H^2} \quad \text{and} \quad \hat{\tau}_s = \frac{kt_s}{H^2}. \tag{4.1}$$

Then the temperature distribution is given by

$$\frac{\partial\theta}{\partial\hat{\tau}} = \frac{\partial^2\theta}{\partial Z^2} + \frac{\alpha^2}{R}\frac{\partial}{\partial R}\left(R\frac{\partial\theta}{\partial R}\right), \quad 0 \leqslant \hat{\tau} \leqslant \hat{\tau}_s, \tag{4.2}$$

subject to the conditions (2.14), (2.15) and

$$\frac{\partial\theta}{\partial Z} \tag{4.3}$$

together with the initial condition (2.12). As $\hat{\tau}_s \ll 1$ (in fact $\hat{\tau}_s = O(\varepsilon)$) the solution is represented by

$$\theta = U_s(R, \hat{\tau})V_s(Z, \hat{\tau}), \tag{4.4}$$

with the radial stratification function $U_s(R, \hat{\tau})$ given as in (2.25) with ε replaced by $\hat{\tau}_s$, and τ replaced by $\hat{\tau}/\hat{\tau}_s$.

The vertical stratification function $V_s(Z, \hat{\tau})$ is governed by

$$\frac{\partial V_s}{\partial\hat{\tau}} = \frac{\partial^2 V_s}{\partial Z^2}, \quad 0 \leqslant \hat{\tau} \leqslant \hat{\tau}_s, \tag{4.5}$$

subject to the boundary conditions

$$\frac{\partial V_s}{\partial Z} = -Bi_2 V_s \quad \text{at} \quad Z = 1, \tag{4.6}$$

$$\frac{\partial V_s}{\partial Z} = Bi_1 V_s \quad \text{at} \quad Z = 0, \tag{4.7}$$

and

$$V_s = 1, \quad 0 \leqslant Z \leqslant 1 \quad \text{at} \quad \hat{\tau} = 0. \tag{4.8}$$

For small τ the solution is given by the composite function

$$V_s(Z,\hat{\tau}) = -1 + \operatorname{erf}\left(\frac{Z}{2\sqrt{\hat{\tau}}}\right) + \exp[Bi_1 Z + Bi_1^2\hat{\tau}] \times \operatorname{erfc}\left(\frac{Z}{2\sqrt{\hat{\tau}}} + Bi_1\sqrt{\hat{\tau}}\right) + \operatorname{erf}\left(\frac{1-Z}{2\sqrt{\hat{\tau}}}\right) + \exp[Bi_2(1-Z) + Bi_2^2\hat{\tau}] \times \operatorname{erfc}\left(\frac{(1-Z)}{2\sqrt{\hat{\tau}}} + Bi_2\sqrt{\hat{\tau}}\right). \tag{4.9}$$

It remains now to consider the solution for the pouring sequence defined by (2.21)–(2.23) with the initial condition:

$$V(Z,\tau) = V_s(Z,\hat{\tau}_s) \quad \text{at} \quad \tau = 0, \quad 0 \leqslant Z \leqslant 1. \tag{4.10}$$

Ladle temperature distribution during pouring $0 \leqslant \tau \leqslant 1$ *with prior thermal stratification.*

To make (2.21)–(2.23) and (4.10) amenable to numerical study introduce the new variable

$$y = Z/(1-\tau)^2. \tag{4.11}$$

The governing equations become

$$\varepsilon\frac{\partial^2 V}{\partial y^2} = (1-\tau)^4\frac{\partial V}{\partial \tau} + 2(y-1)(1-\tau)^3\frac{\partial V}{\partial y}, \quad 0 \leqslant y \leqslant 1, \quad 0 \leqslant \tau \leqslant 1, \tag{4.12}$$

subject to the boundary conditions:

$$\frac{\partial V}{\partial y} = -Bi_2(1-\tau)^2 V \quad \text{at} \quad y = 1, \tag{4.13}$$

$$\frac{\partial V}{\partial y} = Bi_1(1-\tau)^2 V \quad \text{at} \quad y = 0, \tag{4.14}$$

and

$$V = V_s(y,\hat{\tau}_s) \quad \text{at} \quad \tau = 0, \quad 0 \leqslant y \leqslant 1. \tag{4.15}$$

Using the Crank–Nicolson method, see Smith [4], it was a straightforward matter to program these equations. For the jth to $(j+1)$th time step, $(1-\tau)$ was replaced by $(1-\tau_{j+1/2})$, and apart from this the implicit procedure followed that in [4]. In a typical calculation a time step of $\Delta\tau = 0.001$ and spatial step $\Delta y = 0.01$ was employed.

Note that the thermal distribution (4.9) prior to pouring can also be found using the Crank–Nicolson method. This study was completed so as to achieve a single computer programme for the waiting and pouring sequences. In doing so it was necessary (see (4.9)) to use boundary layer type variables of the form $\zeta = Z/2\sqrt{\hat{\tau}}$. The spatial step in ζ was then chosen so as to provide the thermal distribution at $\tau = 0$ for nodal points $y = 0(0.01)\ 1.00$, and so avoided the use of interpolation procedures.

Numerical solutions have been obtained for the dimensionless emptying times $\varepsilon = 0.001$, 0.002 and 0.004. The effect of ladle surface heat transfer was simulated by values $Bi_1 = 0.5$, 1, 3 and 5 first with an insulating slag surface $Bi_2 = 0$ and then allowing for slag surface heat transfer on taking values $Bi_2 = Bi_1/20$. Standing periods $\hat{\tau}_s/\varepsilon = 0(0.25)\ 1.00$ were also investigated so as to simulate thermal stratification prior to the pouring sequence. The results of these numerical studies are considered in the next section.

5. DISCUSSION OF RESULTS AND COMPARISON OF THEORETICAL PREDICTIONS WITH PLANT OBSERVATIONS

It is the purpose of this section to discuss the results of the different methods used to solve this mathematical model for heat transfer and to assess the relevance of these results to plant observations. For the pouring of molten steel, the nozzle pouring temperature T_N is greater than T_F, the fusion temperature. In practice the fusion temperature of molten steel lies in the range 1470 to 1530°C. Furthermore there are variations in the observed initial temperature T_1 (although here an approximate value of 1600°C is employed). Plant data indicates that the dimensionless fusion temperature θ_F usually lies in the range $0.942 \leqslant \theta_F \leqslant 0.957$. Clearly, in the interpretation of the theoretical results, the dimensionless nozzle streaming temperature $(T_N - T_0)/(T_1 - T_0)$ must be greater than this value.

(A) *The case of the insulating slag surface with no initial thermal stratification* $Bi_2 = 0$ *and* $\tau_s = 0$

In Fig. 2 the variation in temperature of the molten steel on the vertical axis is displayed for various values of the dimensionless time τ. These

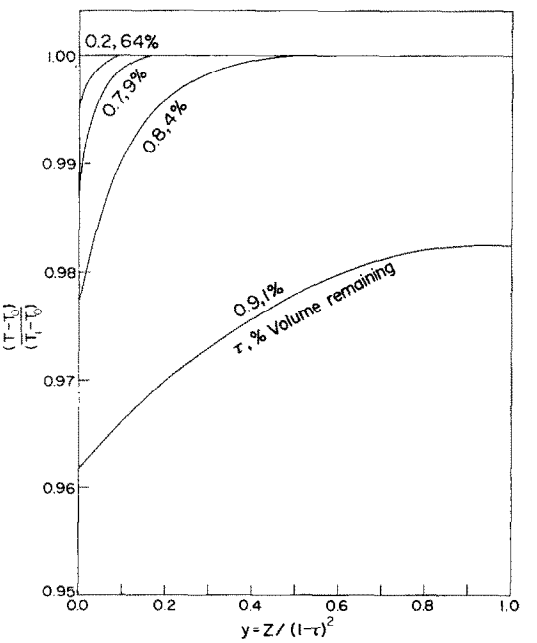

FIG. 2. Dimensionless temperature distribution for various times ($Bi_1 = 5$, $Bi_2 = 0$, $\varepsilon = 0.002$).

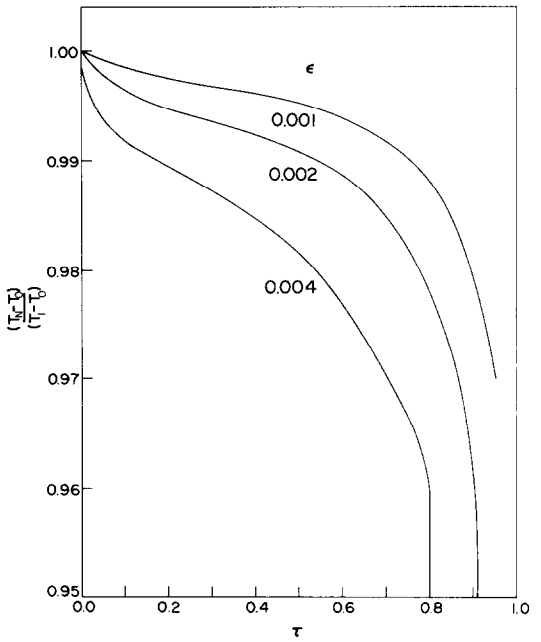

FIG. 3. Dimensionless nozzle streaming temperature against time for various ε ($Bi_1 = 5$, $Bi_2 = 0$).

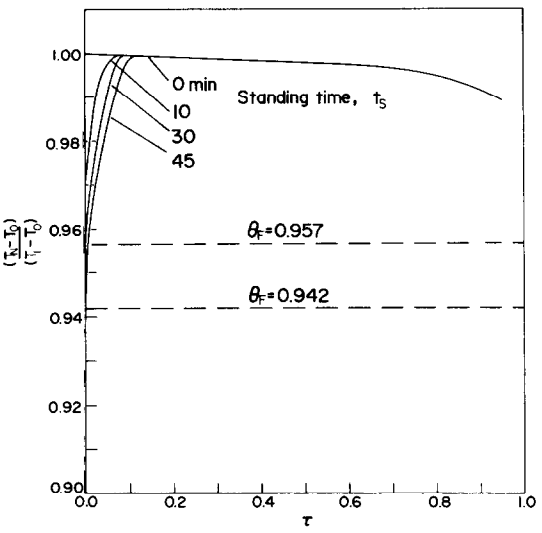

FIG. 4. Dimensionless nozzle streaming temperature against time for various standing times ($Bi_1 = 2$, $Bi_2 = 0$, $\varepsilon = 0.001$).

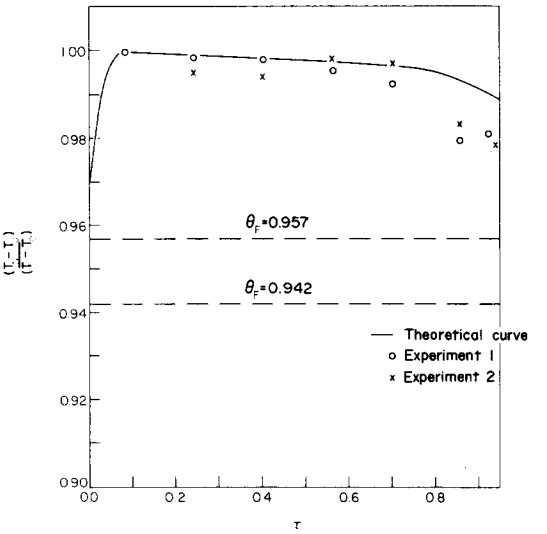

FIG. 5. Theoretical and experimental values of dimensionless nozzle streaming temperature against time ($Bi_1 = 2$, $Bi_2 = 0$, $\varepsilon = 0.001$ standing time equals 30 min).

profiles are valid for the bulk of the steel except in the transient thermal boundary layer region attached to the cylindrical surface. Appreciable changes in temperature, below the initial temperature, only occur for $\tau > 0.85$.

Figure 3 shows the effect on the nozzle streaming temperature of decreasing ε, which is equivalent to increasing the nozzle size. (This is for the case $Bi_1 = 5$.) A decrease in ε implies a faster emptying rate, and hence as shown, a slowing down of the cooling induced by convective heat transfer. It should be noted that the numerical and analytical solutions are in excellent agreement up to $\tau = 1 - O(\varepsilon^{1/3})$, as expected, and consequently only the results for the numerical solutions are displayed.

(B) *The case of an insulating slag surface with initial thermal stratification, $Bi_1 = 2$, $Bi_2 = 0$, $\tau_s \neq 0$*

For $Bi_1 = 2$ and $\varepsilon = 0.001$, nozzle streaming temperatures are displayed in Fig. 4 for initial thermal stratification periods $t_s = 10$, 30 and 45 min. The important feature here is that in each case the thermal stratification region at the base is drained off by the time $\tau = 0.1$. For $\tau > 0.1$ the nozzle temperature in each case will be the same and thus independent of the standing period. Of course, this assumes that the steel is not left standing for so long that actual solidification commences prior to pouring. Using (4.9) it is easy to show that this means

$$\hat{\tau}_s \leqslant \pi/4\left(\frac{1-\theta_F}{Bi_1}\right)^2. \tag{5.1}$$

For the typical ladle considered this corresponds to $t_s = 29$ min. However, the thermal capacity of the ladle wall, and the associated transient behaviour, which have not been included in this preliminary model, would affect this conclusion.

(C) *Comparison of theoretical predictions with plant observations*

Figure 5 shows the non-dimensional nozzle temperature variation observed throughout a typical pouring sequence. Such temperature observations are very difficult to make during the first few minutes of pouring. In fact sometimes the steel does indeed solidify in the nozzle itself. This indicates that the temperature may in fact be lower than the observed value. In view of the difficulty of making observations, and the variations between the two casts illustrated, the agreement with the theoretical model is satisfactory.

6. CONCLUSIONS

An inviscid flow model for heat transfer in the pouring sequence of a ladle of molten steel has been employed to obtain the nozzle streaming temperature for a typical ladle. The main limitations of the model are firstly, that the idealization of the wall thermal boundary condition neglects the thermal capacity of the wall and the associated transient behaviour; secondly, that near the end of the pouring sequence the inviscid flow assumption is invalid.

Further three dimensional numerical studies to remove the first of these limitations are now in progress.

Acknowledgements—One of us (P.E.) is indebted to the Science Research Council for a maintenance grant. We are indebted to Mr. V. J. Small (British Steel Corporation (Scunthorpe)) for his continued interest in this problem.

REFERENCES

1. J. W. Hlinka, Water model for the quantitative simulation of heat and fluid flow in liquid steel refractory systems, Homer Research Laboratory, Bethlehem Steel Corporation, U.S.A. (1976).
2. J. Szlekely and R. G. Lee, The effect of slag thickness on heat loss from ladles holding molten steel, *Trans. A.I.M.E.* **242**, 961–965 (1968).
3. H. S. Carslaw and J. C. Jaeger, *Conduction of Heat in Solids*, Oxford University Press, Oxford (1947).
4. G. D. Smith, *Numerical Solution of Partial Differential Equations*, Oxford University Press, Oxford (1965).

ETUDE THEORIQUE DU TRANSFERT THERMIQUE DANS UNE LINGOTIERE D'ACIER LIQUIDE PENDANT LA COULEE

Résumé—On propose un modèle théorique pour l'écoulement et le transfert de chaleur d'un acier liquide durant la coulée d'une lingotière. On obtient des solutions analytique et numérique. Dans les limites du modèle, un accord satisfaisant est constaté avec les observations.

THEORETISCHE UNTERSUCHUNG DES WÄRMEÜBERGANGS IN EINER GUSSPFANNE MIT GESCHMOLZENEM STAHL WÄHREND DES GIESSENS

Zusammenfassung—Für die Strömung und den Wärmeübergang einer Stahlschmelze in der Gußpfanne während des Gießens wird ein theoretisches Modell vorgeschlagen. Analytische und numerische Lösungen wurden gewonnen. Innerhalb der Grenzen des Modells ist die Übereinstimmung mit Betriebserfahrungen befriedigend.

ТЕОРЕТИЧЕСКОЕ ИССЛЕДОВАНИЕ ТЕПЛОПЕРЕНОСА В КОВШЕ С РАСПЛАВЛЕННОЙ СТАЛЬЮ ПРИ РАЗЛИВКЕ

Аннотация — Предложена теоретическая модель течения и теплопереноса расплавленной стали в ковше при разливке. Получены аналитические и численные решения. В пределах ограничений модели результаты расчётов удовлетворительно согласуются с данными наблюдений, полученными в промышленных условиях.